JOURNAL OF VIROLOGY, Dec. 1979, p. 860-875
0022-538X/79/12-0860/16$02.00/0

Vol. 32, No. 3

Restriction Endonuclease Mapping of Unintegrated Proviral DNA of Snyder-Theilen Feline Sarcoma Virus: Localization of Sarcoma-Specific Sequences

CHARLES J. SHERR,* LOUIS A. FEDELE, LUDVIK DONNER, AND LUBOMIR P. TUREK

Laboratory of Viral Carcinogenesis, National Cancer Institute, Bethesda, Maryland 20205

Received for publication 29 May 1979

Extrachromosomal DNA purified from mink cells acutely infected with the Snyder-Theilen strain of feline sarcoma virus (FeSV) was digested with restriction endonucleases, and the DNA fragments were electrophoretically separated, transferred to a solid substrate, and hybridized with radiolabeled DNA transcripts complementary to different portions of the FeSV RNA genome. Major DNA species 8.4 and 5.0 kilobase pairs (kbp) long represent the linear, unintegrated proviruses of Snyder-Theilen feline leukemia virus and FeSV, respectively. Transfection experiments performed with electroeluted DNAs showed that the 8.4-kbp form led to the production of replicating nontransforming virus in mink and cat cells; in contrast, the 5.0-kbp DNA produced helper virus-independent foci of transformation in mouse NIH/3T3 cells and helper virus-dependent foci in mink cells at an efficiency comparable to that obtained with unfractionated extrachromosomal DNA. Sites of restriction endonuclease cleavage for six enzymes were oriented with respect to one another within the FeSV provirus. *Eco*RI recognized cleavage sites at 0.3 to 0.4 kbp from each terminus of FeSV DNA, reducing the 5.0-kbp DNA to molecules 4.3 kbp long; this enzyme excised a large internal proviral DNA fragment of corresponding size from the DNA of FeSV-transformed mink nonproducer cells. By using DNA transcripts complementary to different portions of the FeSV genome, sarcoma-specific sequences (the FeSV *src* gene) were positioned within 2.1 and 3.4 kbp from the 5′ end of the proviral DNA with respect to the viral RNA genome. The *src* gene is flanked at both ends by sequences shared in common with feline leukemia virus. The localization of *src* sequences to this region suggests that a portion of an FeSV polyprotein which contains feline oncornavirus-associated cell membrane antigen (FOCMA-S) is the major product of this gene.

Mammalian type C sarcoma viruses cause solid tumors in animals and morphologically transform fibroblastic and epithelioid cells in tissue culture. Like other mammalian sarcoma viral isolates, the feline sarcoma virus (FeSV) is replication defective and requires a replication-competent helper virus for growth. Three independent isolates of FeSV have been obtained from naturally occurring tumors in association with feline leukemia virus (FeLV). These include the Snyder-Theilen (ST) (38), Gardner-Arnstein (15), and McDonough (24) strains, all of which differ from one another in certain of their biological properties (27).

The RNA genomes of each of the three FeSV strains are composed of two operationally distinct subsets of nucleic acid sequences (13). These include sequences shared in common with their natural FeLV helper virus (designated *com* sequences), as well as other gene sequences unique to the sarcoma virus (designated *src*), which are presumed to confer the property of morphological transformation. Genes related to both FeSV *src* and FeSV(FeLV) *com* sequences can be detected in cellular DNA of normal cats and are transmitted like other cellular genes. Although *src*-related sequences are found in all of the Felidae (13), sequences related to *com* are detected only in Mediterranean *Felis* species (5). Of particular interest is the observation that the *src* element of the McDonough strain of FeSV shows no homology to the analogous genes of either ST-FeSV or the Gardner-Arnstein strain of FeSV, both of which share homologous *src* genes (13). Thus, FeSV genomes appear to have been derived by recombinational events between FeLV-specific sequences and cellular *src* elements, at least two of which can be identified in the DNA of normal cat cells.

Some of the *com* sequences of the different

FeSV strains code for antigens related to FeLV *gag* gene products (21, 27, 34, 40). By analogy to FeLV, these sequences are presumed to be located at the 5′ end of FeSV RNA (44). FeSV also encodes a novel antigen, the feline oncornavirus-associated cell membrane antigen (FOCMA-S) (35, 37), which shows no antigenic relationship to known FeLV structural proteins (34, 35, 40). FOCMA-S is expressed on the surfaces of cells transformed by FeSV. A cross-reactive antigen (FOCMA-L) can be detected on lymphoid tumor cells induced by FeLV, but not on untransformed FeLV-infected fibroblasts (11, 37). Antibodies to FOCMA confer resistance against tumor development induced by viruses of the FeSV(FeLV) complex, as demonstrated in natural field studies or with experimentally inoculated animals (11). Recent observations indicate that FeSV codes for a polyprotein containing both *gag* and FOCMA antigenic determinants (34, 35, 40), further suggesting that gene sequences encoding FOCMA-S may be adjacent to *gag* gene sequences in FeSV RNA. The observations that FOCMA expression correlates with viral transformation and that FOCMA is not antigenically related to FeLV structural proteins both raise the possibility that FOCMA-S is encoded by FeSV *src* sequences.

To date, neither the complexity nor the localization of *src* and *com* sequences in FeSV genomes is understood. To approach these questions, we used unintegrated FeSV proviral DNA as a substrate and developed a restriction endonuclease map of the ST-FeSV provirus. FeSV DNA restriction fragments were electrophoretically separated from one another, transferred to nitrocellulose filters, and hybridized to radiolabeled complementary DNA (cDNA) transcripts representing different portions of the FeSV RNA genome (39). The results show that ST-FeSV *src* sequences are located at the center of the FeSV linear DNA provirus and are flanked by *com* sequences at both the 5′ and 3′ termini.

MATERIALS AND METHODS

Viruses and cells. The ST strain of FeSV(FeLV) was generously provided by Arthur Frankel, Laboratory of Viral Carcinogenesis, National Cancer Institute, and was grown in mink Mv1Lu cells (American Type Culture Collection CCL64). CCC clone 81 cat cells containing the S^+L^- Moloney sarcoma virus genome (12) were a gift from Peter Fischinger, Laboratory of Viral Carcinogenesis, National Cancer Institute. FeSV-transformed nonproducer rat cells (F3 NRK clone 2) infected with the mouse type C virus AT-124 (42) were used as a source of FeSV pseudotype virus, as previously described (34). For synthesis of cDNA transcripts, viruses harvested at 12-h intervals from chronically infected cells were clarified of cellular debris, pelleted, and banded isopycnically in sucrose ($\rho \sim 1.16$) as previously described (4). For acute infection of cells before purification of extrachromosomal DNA, mink cells seeded at 70% confluency were infected for 24 h with unconcentrated, virus-containing medium from chronically producing cultures in the presence of 10 μg of polybrene per ml (43). To obtain a multiplicity of 0.5 to 1.0 focus-forming units per cell, overnight harvests from 20 890-cm^2 roller bottles (~50 ml/roller) were used to infect 10 roller bottles of subconfluent cells.

Virus titration and UV inactivation. Focus-forming titers of FeSV were determined in mink Mv1Lu cells, and the replicating helper virus titer was routinely estimated by indirect focus formation in S^+L^- Moloney murine sarcoma virus-infected cat cells, CCC clone 81 (12). The cells were infected in the presence of 10 μg of polybrene per ml, and foci were enumerated after 7 days in mink cells and after 9 to 10 days in S^+L^- cells. The titer of freshly harvested, filtered FeSV stock was approximately 3×10^5 FeSV focus-forming units per ml in mink cells and 5×10^5 S^+L^- focus-forming units per ml in CCC clone 81 cells. The ratio of transforming FeSV to replicating FeLV was determined in a replica-plating experiment, in which the ST-FeSV(FeLV) mixed virus stock was used to infect Mv1Lu cells at terminal dilution in microtiter plates. Individual wells were then scored for the presence of transformed cells, and the media were tested for replicating helper virus production in CCC clone 81 cells. The ratio of transforming FeSV to replicating FeLV was estimated to be about 1:4. The natural helper of ST-FeSV(FeLV) was derived from a virus-producing well at terminal dilution. ST-FeSV-transformed nonproducer mink cells were subcultured from single focus-containing wells, and the absence of replicating virus in culture supernatants was determined both by titration in CCC clone 81 cells and by a supernatant reverse transcriptase test (33).

UV inactivation was carried out by the method of Nomura et al. (26), with slight modifications. A 24-h virus harvest was filtered through a 0.2-μm pore size filter, buffered with HEPES (*N*-2-hydroxyethylpiperazine-*N*′-2-ethanesulfonic acid), pH 7.3, at a final concentration of 50 mM, and inactivated under a Mineralight 251 UV lamp (UV Products Inc., San Gabriel, Calif.) at an incident flow rate of approximately 33 ergs · $mm^{-2} \cdot s^{-1}$. The irradiation was carried out with 10 ml of virus stock in a watch cover glass (diameter, 22 cm) under constant agitation. Samples were aspirated directly from the cover glass at time zero and after indicated intervals. The titers of surviving focus-forming FeSV and replicating FeLV were assayed in Mv1Lu and CCC clone 81 cells as described above. The inactivation curves were derived by the least-squares method from a plot of the natural logarithm of the surviving fraction versus time of irradiation. The 37% survival doses were calculated as the inverted values of the slope constants of these curves. Individual foci of mink cells transformed by UV-irradiated FeSV(FeLV) were subcultured.

Determination of RNA genome size. Chronically infected mink cells were pulsed for 24 h with ^{32}P-labeled phosphoric acid, and radiolabeled virus was used as a source of high-molecular-weight ~60S viral RNA (30). ^{32}P-labeled viral RNA was concentrated

under ethanol and suspended and heated for 2 min at 100°C in 0.05 M Tris-hydrochloride, pH 7.8, containing 10% formamide to denature the genomic subunits. Viral subunits were then electrophoresed in 0.5% acrylamide-1% agarose composite gels containing 10% formamide in the presence of ^{3}H-labeled 28S and 18S ribosomal RNA markers (Schwarz/Mann), as described previously (33).

Preparation of cDNA transcripts. ^{32}P-labeled cDNA was synthesized in 50- to 250-μl exogenous reactions performed for 30 min at 41°C (linear kinetics). Each 50 μl contained 0.5 μg of FeSV(FeLV) 50S to 60S RNA, 50 μg of calf thymus DNA primer (length, 10 to 20 nucleotides), 15 U of avian myeloblastosis virus polymerase (Office of Resources and Logistics, National Cancer Institute), and 100 μg of actinomycin D. Reaction mixtures contained 50 mM Tris-hydrochloride, pH 7.8, 50 mM KCl, 8 mM $MgCl_2$, 2 mM dithiothreitol, 0.1 mM each dATP, dGTP, and dTTP, and 100 to 200 μCi of [^{32}P]dCTP (New England Nuclear Corp.; NEG 013X; specific activity, 300 to 400 Ci/mmol). ^{3}H-labeled cDNA was synthesized by the same method except that 10-fold-concentrated [^{3}H]TTP (10 mCi/ml; New England Nuclear Corp.; NET 221X; specific activity, 40 to 60 Ci/mmol) was employed and 0.1 mM unlabeled dCTP was included in reaction mixtures instead of dTTP. Reactions were terminated by the addition of an equal volume of solution containing 100 mM EDTA, 1% sodium dodecyl sulfate, and 1 mg of proteinase K per ml (20 min at 41°C).

Reaction products were diluted to 5 ml in 0.05 M Tris-hydrochloride, pH 7.8, containing 0.1 M NaCl, extracted with 1 volume of phenol-chloroform-isoamyl alcohol (25:24:1) (PCI), treated for 10 min at 65°C with 0.25 N NaOH, neutralized, and concentrated under ethanol. Single-stranded cDNA products were separated from calf thymus primer and unincorporated nucleotide triphosphates by gel filtration on G-50 fine Sephadex (Pharmacia, Uppsala, Sweden). After ethanol precipitation, the yield of cDNA (specific activity, 4×10^8 to 6×10^8 cpm/μg for ^{32}P and 2×10^7 cpm/μg for ^{3}H) was generally 0.2 μg/0.5 μg of viral RNA.

Sequences representing the FeSV genome (designated $cDNA_{rep}$) were obtained by hybridizing total FeSV(FeLV) cDNA to purified RNA obtained from FeSV(AT-124) pseudotype virions. Hybridizations were performed in a solution containing 0.01 M Tris-hydrochloride, pH 7.6, 1 mM EDTA, 0.05% sodium dodecyl sulfate, and 0.75 M NaCl at 68°C by using ratios of FeSV RNA to cDNA of ~10 (final C_rt, 400 mol·s/liter). cDNA-RNA hybrids were separated from single-stranded cDNA on hydroxyapatite at 60°C (7), and duplexes were treated with alkali, neutralized, and concentrated under ethanol. cDNA sequences shared in common between FeSV and FeLV ($cDNA_{com}$) were recovered after a second cycle of hybridization with RNA obtained from FeLV strain F422 grown in cat cells. Hybridizations were performed at 65°C in 0.75 M NaCl by using a 100-fold excess of FeLV RNA over cDNA (final C_rt, 20 mol·s/liter). The reaction products were treated with the single strand-specific nuclease S1 (2) under stringent conditions (4), extracted with PCI, alkali treated, neutralized, and concentrated under ethanol.

Sequences unique to FeSV ($cDNA_{src}$) were prepared by hybridizing FeSV(FeLV) cDNA to FeLV RNA under conditions of reduced stringency (1.5 M NaCl, 60°C). Two selections effectively eliminated more than 99% of those cDNA sequences which hybridized to FeLV RNA and resulted in 10% of the cDNA fractionating as single strands on hydroxyapatite. The cycled single-stranded cDNA was then reannealed to FeSV (AT-124) RNA under more stringent conditions (68°C, 0.65 M NaCl), and hybrids recovered on hydroxyapatite at 60°C were alkali treated, neutralized, and concentrated under ethanol. The final yield of cDNA *src* was 2% of the starting FeSV(FeLV) cDNA.

Transcripts complementary to the extreme 5′ end of FeSV(FeLV) RNA ("strong stop DNA") were synthesized exactly as described by Haseltine et al. (17). Endogenous syntheses were performed with detergent-disrupted virions in a final reaction volume of 0.5 ml by using 4 μM labeled substrate and each of the other unlabeled nucleoside triphosphates at 1 mM. Exogenous syntheses were performed by using 2 μg of 60S FeSV(FeLV) RNA as template, no exogenous primer, and 15 U of avian myeloblastosis virus polymerase in a final reaction volume of 0.2 ml; the concentrations of all other reagents were identical to those used in endogenous reactions. After chromatography on Sephadex G-50, the majority of the labeled product was digested with alkali, neutralized, and electrophoresed in 10% polyacrylamide slab gels containing 5 M urea. As a control, the remainder of the product was electrophoresed without alkali digestion to determine the relative mobility of strong stop DNA linked to endogenous tRNA primer. A denatured *Hae*III digest of ΦX174 replicative-form DNA (Bethesda Research Laboratories, Bethesda, Md.) was used to calibrate the gels. The strong stop cDNA (~140 bases long) was identified by autoradiography; the region of the gel containing the labeled DNA band was excised, and the DNA was eluted, extracted with PCI, and concentrated under ethanol. Approximately 10 to 15% of the DNA synthesized in endogenous reactions was detected as strong stop cDNA, whereas only ~5% of the cDNA synthesized in exogenous reactions migrated as this species. However, the final yield of labeled product in the latter reactions was approximately fivefold greater. Both $cDNA_{5'}$ preparations hybridized to approximately 65% at saturation to FeSV(FeLV) RNA when S1 nuclease was used to detect hybrids (2, 4), and the two preparations gave similar results when annealed to FeSV DNA restriction fragments (see below).

Polyadenylic acid [poly(A)]-selected FeSV(FeLV) RNA was used to prepare cDNA transcripts complementary to the 3′ end of viral RNA ($cDNA_{3'}$). Viral 50S to 60S RNA was thermally lysed in 0.05 M Tris-hydrochloride, pH 7.8, at 100°C for 5 min and sedimented in 15 to 30% neutral sucrose gradients (SW41 rotor; 38,000 rpm; 14 h). RNA fractions 12S to 18S in size were pooled, concentrated, and twice chromatographed on oligodeoxythymidylic acid-cellulose (type I; Collaborative Research, Waltham, Mass.) as described previously (45). Poly(A)-containing RNA was

resedimented in neutral sucrose, and 12S to 18S RNA fractions were again pooled and concentrated under ethanol. Poly(A)-containing RNA was used as a template in standard synthetic reactions performed with calf thymus primer. The specific activity of these transcripts (designated $cDNA_{3'}$) was $\sim 3 \times 10^8$ cpm/μg. $cDNA_{3'}$ hybridized to a final extent of 73% to total FeSV(FeLV) poly(A)-containing RNA but to less than 7% saturation with poly(A)-negative 12S to 18S viral RNA.

Characterization of labeled cDNA transcripts. With the exception of $cDNA_{5'}$, cycled cDNA transcripts were all 5S to 8S in size, as determined by sedimentation in alkaline sucrose gradients. FeSV $cDNA_{rep}$ hybridized to a final extent of more than 90% with RNAs from FeSV(FeLV) and FeSV(AT-124) when stringent conditions (0.75 M Na^+, 65°C) and S1 nuclease were used to detect hybrids (4). FeSV $cDNA_{com}$ hybridized to a final extent of 84% with RNA from FeSV(FeLV) and to 80% with RNAs from FeSV(AT-124) and FeLV itself. FeSV $cDNA_{src}$ hybridized to 68% with both FeSV(FeLV) and FeSV(AT-124) RNA, but to less than 2% with FeLV RNA (at a C_rt of >20 mol·s/liter). All cDNA transcripts were more than 98% sensitive to digestion with S1 nuclease and chromatographed only as single strands on hydroxyapatite. The midpoints of thermal denaturation curves of hybrids formed with FeSV(FeLV) RNA were all greater than 80°C.

Kinetic experiments (C_rt analyses) performed with the various cDNA's confirmed their sequence specificity and permitted retrospective studies of the purity and content of viral RNAs used to prepare transcripts. The $C_rt_{1/2}$ obtained with [^{32}P]$cDNA_{src}$ and FeSV(FeLV) RNA (0.2 mol·s/liter) was fivefold greater than the $C_rt_{1/2}$ obtained with $cDNA_{com}$ (0.04 mol·s/liter). Similar results were obtained with [^{3}H]$cDNA_{com}$ in double-label experiments performed with [^{32}P]$cDNA_{src}$, showing that the ratio of FeLV to FeSV RNA genomes in the RNA preparations used to prepare transcripts was approximately 5:1. Given that the size of the FeLV genome is approximately twofold greater than that of FeSV RNA (see below), a 2% yield of $cDNA_{src}$ was not unexpected.

The complexity of ^{32}P-labeled transcripts employed in these studies was not directly determined. First, we were not able to obtain an adequate source of purified, labeled FeSV RNA free of helper viral genomes, nor did we choose to use a "cDNA excess" hybridization method since the specific activities of the transcripts were so high and the quantities of radioactive cDNA required for such studies would be too great. By using ^{3}H-labeled FeLV cDNA transcripts synthesized under the same conditions as those used to prepare [^{32}P]-cDNA, protection experiments (4) were performed with ^{32}P-labeled FeLV RNA and RNase to detect hybrids. These latter studies showed that the transcripts were representative of the entire FeLV genome (63 and 85% protection at molar ratios of RNA to cDNA of 1 and 4, respectively). Thus, we concluded that under the conditions used to detect DNA restriction fragments on nitrocellulose (cDNA excess), all fragments containing sequences present in the [^{32}P]cDNA should be scored, and the degree of hybridization obtained with various, specific cDNA's should reflect the sequence composition of the various DNA fragments (see below).

Preparation of proviral DNA. Extrachromosomal DNA containing the FeSV provirus was purified by chromatography on hydroxyapatite (36). In brief, mink cells infected with FeSV(FeLV) for 24 h were lysed in 8 M urea–1% sodium dodecyl sulfate–10 mM EDTA in 0.24 M phosphate buffer, pH 6.8, and the lysate was centrifuged at 80,000 × *g* maximum for 60 min to sediment high-molecular-weight DNA. After reextraction of the pellet, the pooled supernatant fractions were applied to hydroxyapatite equilibrated with the lysing solution. After washing with 8 M urea–0.24 M phosphate buffer to remove protein and RNA, the column was sequentially eluted with 0.14 M phosphate and 0.5 M phosphate buffer, both pH 6.8. Double-stranded extrachromosomal DNA, delivered in the 0.5 M phosphate elution, was reconcentrated on hydroxyapatite, dialyzed against 0.01 M Tris-hydrochloride–2 mM EDTA, and concentrated under ethanol. The ratios of absorbance at 260 nm to absorbance at 280 nm for purified DNA were greater than 1.9, and the yield was less than 1% of the total cell DNA. In general, 5 to 15 μg of DNA was recovered per 890-cm^2 roller bottle infected at 70% confluency. Total extrachromosomal DNA was electrophoresed on 1% agarose gels (39), and DNA corresponding to the FeLV and FeSV linear proviruses was recovered by electroelution (23), extracted with PCI, and concentrated by ethanol precipitation.

Infectious DNA assay. The biological activity of FeSV(FeLV) DNA was determined by the calcium precipitate method of Graham and van der Eb (16). Recipient cells were seeded at 5×10^5 cells per well in six-well cluster dishes (diameter, 35 mm) 24 h before DNA infection. Extrachromosomal DNA was diluted in HEPES-buffered saline, pH 6.95, the lowest pH allowing the formation of a fine DNA-calcium precipitate (22). Sheared NIH/3T3 cell DNA at 20 μg/ml was used as a carrier (22). Calcium chloride was added to a final concentration of 0.125 M. The coprecipitate was allowed to form for 20 to 25 min at room temperature, resuspended by pipetting, and inoculated in appropriate recipient cultures. After 4 h the cells were treated for 4 min with 17.5 to 25% glycerol in HEPES-buffered saline (10) by the procedure of Stow and Wilkie (41). HEPES-buffered saline, pH 7.1, was used at this step since it proved to have a less toxic effect on the cells.

The replicating FeLV helper activity of proviral DNA was detected (i) by S^+L^- focus formation at 14 to 17 days after direct transfection of CCC clone 81 cat cells and (ii) by transfection of uninfected Mv1Lu mink cells followed by CCC clone 81 assays of infectious helper virus in the culture supernatants at 2 and 4 weeks after transfection. These procedures could be employed either for total FeSV(FeLV) extrachromosomal DNA or for DNA species obtained by electroelution. In contrast, the capacity to transform uninfected mink cells was poor when total FeSV(FeLV) DNA was used and was undetectable when electroeluted DNA species were used. In the few cases where foci of transformation were observed when total extra-

chromosomal DNA was used, all cultures were found to be producing infectious FeSV(FeLV). Thus, detectable focus formation in mink cells after transfection with FeSV DNA appeared to require the presence of a replicating helper virus. To detect transforming FeSV proviral DNA in mink recipient cultures, the cells were infected with FeLV for 18 h immediately after glycerol treatment in the presence of 10 μg of polybrene per ml. A low multiplicity of FeLV infection (0.01 infectious units per cell, as determined in CCC clone 81 cells) was used to facilitate the gradual spread of helper virus in recipient cultures. The multiplicity of helper virus infection was empirically determined to permit maximal spread of FeSV to uninfected cells without the rapid establishment of viral interference. This procedure, then, could be used to score for the presence of transforming FeSV provirus at 3 to 4 weeks after transfection with both unfractionated and electroeluted DNA preparations. Helper-independent transformation with FeSV DNA was determined in mouse NIH/3T3 recipient cultures (22). Foci of FeSV DNA-transformed NIH/3T3 cells were observed 17 to 21 days after transfection. Randomly selected foci were subcultured and tested for the presence of rescuable FeSV genomes by superinfection with a dual-tropic mouse helper virus. The transforming capacity of the rescued virus was determined in Mv1Lu mink cells.

Where stated, the specific infectivity of DNA preparations was titrated by the endpoint dilution method (9). Fourfold DNA dilutions were inoculated in triplicate recipient cultures, and the 50% infectious dose (equals 1 infectious unit) was calculated as described previously (28). The specific infectivity is expressed in infectious units per microgram of DNA. Since quantities of fractionated DNAs could not be determined due to the presence of the NIH/3T3 carrier DNA used during electroelution, the microgram values were standardized to the quantities of unintegrated DNA applied to gels. The infectious DNA titers may be underestimated in those cases where a clear-cut dilutional endpoint was not reached.

Restriction endonuclease digestions. *Eco*RI was purchased from Boeringer Mannheim Corp., (Indianapolis, Ind.); *Bam*HI, *Bgl*II, *Hin*dIII, *Hae*III, and *Kpn*I were from Bethesda Research Laboratories; and *Xho*I and *Sal*I were from New England Biolabs, Beverly, Mass. Linear FeSV proviral DNA, purified by electroelution, was digested to completion in the presence of bacteriophage λ DNA (Bethesda Research Laboratories). Digestions with each enzyme were performed under the conditions recommended by the manufacturers. For dual digestions with enzymes requiring high-salt buffers (*Bam*HI, *Eco*RI, *Xho*I, and *Sal*I), the two enzymes were added simultaneously in a high-salt buffer containing 50 mM Tris, pH 7.8, 100 mM NaCl, 7 mM $MgCl_2$, and 2 mM β-mercaptoethanol. For dual digestions requiring low-salt conditions (*Bgl*II, *Kpn*I), enzymes were added simultaneously in a low-salt buffer containing 20 mM Tris, pH 7.4, 7 mM $MgCl_2$, 2 mM β-mercaptoethanol, and 20 μg of nuclease-free bovine serum albumin (Bethesda Research Laboratories) per ml. Dual digestions with *Kpn*I or *Bgl*II and a second enzyme requiring high salt were performed sequentially; after digestion in low-salt buffer, the concentrations of Tris-hydrochloride and NaCl were adjusted to high-salt buffer conditions, and the second enzyme was added. All digestions were performed for 5 h at 37°C, using a twofold excess of enzyme units over substrate.

Electrophoresis, transfer, and hybridization. The method was that described by Southern (39), as modified by others (32). In brief, restriction fragments (~0.3 μg of extrachromosomal DNA per slot or 10 μg of cellular DNA per slot) were separated electrophoretically on 0.8 to 1.2% agarose gels, stained with ethidium bromide, and visualized under UV light. Bacteriophage λ fragments were used to calibrate the gels; fragment sizes are given in kilobase pairs (kbp). After transfer of fragments and fixation to nitrocellulose sheets (0.45 μm; Schleicher & Schuell Co., Keene, N.H.), the filters were preannealed at 41°C for 18 h in buffer containing 50% formamide, 0.02% each polyvinyl pyrrolidone, bovine serum albumin, and Ficoll 400, 0.05 M HEPES buffer, 3× SSC (1× SSC is 0.15 M sodium chloride plus 0.015 M sodium citrate) and 25 μg of sheared 5S denatured mink DNA per ml. Filters were then hybridized in the same solution containing 0.5×10^6 to 5.0×10^6 cpm of [^{32}P]cDNA per ml for 24 to 48 h, washed, dried, and subjected to autoradiography at −70°C (20, 32). Positions of bands were determined by measurement, using ^{14}C-labeled ink to define the electrophoretic origins and boundaries of the papers. After correction for shrinkage of the papers, the calibration of autoradiographically visualized bands was reproducible to standard deviations of ±4% for fragments in the size range of 0.7 to 5.0 kbp.

Under the above described conditions, DNA fragments of <0.7 kbp were found to bind poorly to nitrocellulose. To study DNA fragments of this size, fragments were electrophoresed in 1.6% agarose and were transferred covalently to activated Whatman papers as described previously (J. C. Alwine, D. J. Kemp, B. A. Parker, J. Reiser, J. Renart, G. Stark, and G. M. Wahl, Methods Enzymol., in press). The latter papers were preannealed in a solution containing ~1 mg of salmon sperm DNA per ml, 0.1 M glycine, 5× SSC, and all other components as described above. The conditions of hybridization, washing, and autoradiography were identical to those used for nitrocellulose papers.

Quantitation of radiographs. Where applicable, the relative intensities of autoradiographic bands were estimated as follows. Samples containing 0.6 μg of DNA were digested with endonucleases as indicated, divided into equal portions and run in duplicate on the left and right sides of the same gel. After transfer, the papers were cut in half and were separately hybridized with two different [^{32}P]cDNA's of identical specific activity. Autoradiographs were developed and cut into strips corresponding to individual gel lanes. The film strips were then scanned at 590 nm with a Gilford densitometer and recorder adjusted so that the most intense band gave ~100% deflection of the recording pen. The areas under the peaks of the densitometer traces were estimated by weighing the papers on a balance accurate to 0.1 mg. Intensity units (in milligrams) recorded for each film strip were summed, and the total intensity was normalized to 100 in order to allow a quantitative comparison of separate determi-

nations from different experiments. Intensities are expressed as milligrams per cent in the tables to indicate the contribution of each autoradiographic band to the total intensity observed. The relative intensity was calculated by dividing the normalized intensity units obtained for each fragment by the length of the fragment in kilobase pairs. Experiments with $cDNA_{rep}$ showed that the band intensity of all FeSV DNA fragments in a single lane was principally a function of fragment size (±20%) for fragments between 5.4 and 1.0 kbp long. Thus, the relative intensities of bands obtained with transcripts representing different portions of the FeSV genome could be used to quantify the contribution of *src*-, *com*-, 5'-, and 3'-derived sequences in each restriction fragment.

RESULTS

Determination of FeSV and FeLV genome sizes. Although the exact mechanism is unclear, UV irradiation appears to inactivate RNA tumor virus genomes at a rate directly proportional to size (6, 14, 26). Using this approach, we compared the relative target sizes of transforming ST-FeSV and its natural FeLV helper. The titers of the surviving fractions in virus stocks irradiated for different periods of time were determined by direct focus formation in mink Mv1Lu cells for transforming FeSV and by indirect focus formation in CCC clone 81 cat cells for replicating FeLV. The latter cell line contains the integrated S^+L^- Moloney murine sarcoma DNA provirus and undergoes "super-transformation" when infected by a variety of helper viruses, including FeLV (12). Figure 1 shows the UV survival curves obtained for FeSV and FeLV. The 37% survival doses for FeSV and FeLV were 1,887 ± 63 and 1,051 ± 146 ergs/mm^2, respectively. Thus, the relative target size of FeSV was 56 ± 10% that of the FeLV genome.

From three different experiments, a total of 26 foci were selected at random from mink cell cultures infected with UV-irradiated virus stocks under conditions in which the surviving fraction was between 5×10^{-3} and 1×10^{-4} of the initial focus-forming titer. The transformed cells were grown up, and the media of cultures were tested for the presence of infectious virus in CCC clone 81 cells. As expected from the preferential inactivation of FeLV versus FeSV genomes (Fig. 1), all of the transformed clones were negative for virus production. Infection of each of the transformed nonproducer clones with FeLV gave rise to virus which led to foci of transformation of Mv1Lu mink cells. Restriction endonuclease analyses performed with the cellular DNA of 15 of these nonproducer clones also showed that they contained full-length FeSV proviral DNA (see below for representative results). These experiments showed, then, that the great majority of transformed clones derived after extensive UV irradiation contained rescuable, biologically nondefective FeSV genomes.

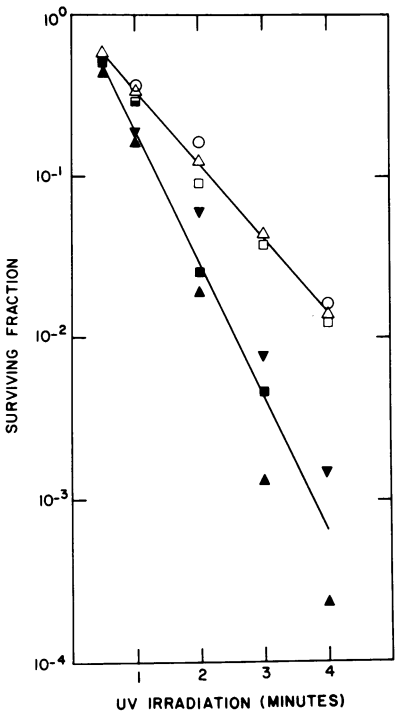

FIG. 1. *Comparison of the relative UV target sizes of transforming ST-FeSV and its natural helper virus. Virus stocks irradiated at an incident flow rate of 2,000 ergs/mm^2 per min for various periods of time were titrated for direct (FeSV) and indirect (FeLV) focus formation by using Mv1Lu mink and CCC clone 81 cat cells, respectively. Data from three experiments are shown. The exponential inactivation curves were estimated by the least-squares method, and 37% survival doses were calculated from the slope constants. Symbols: ○, △, and □, surviving fraction of transforming FeSV; ▲, ▼, and ■, surviving fraction of replicating FeLV.*

To directly measure the sizes of FeSV and FeLV RNA subunits, ^{32}P-labeled FeSV(FeLV) 60S RNA was thermally denatured and electrophoresed in agarose-acrylamide composite gels in the presence of formamide. Two classes of subunits corresponding to 32S and 26S RNA species were resolved (Fig. 2). Estimation of molecular weights by comparison to [^3H]rRNA markers suggested that the chain lengths of these species were approximately 7.5 and 4.3 kilobases, respectively, which is in good agreement with the expected relative target sizes of FeLV and FeSV genomes.

Analysis of FeSV(FeLV) proviral DNA. Total extrachromosomal DNA obtained 24 h

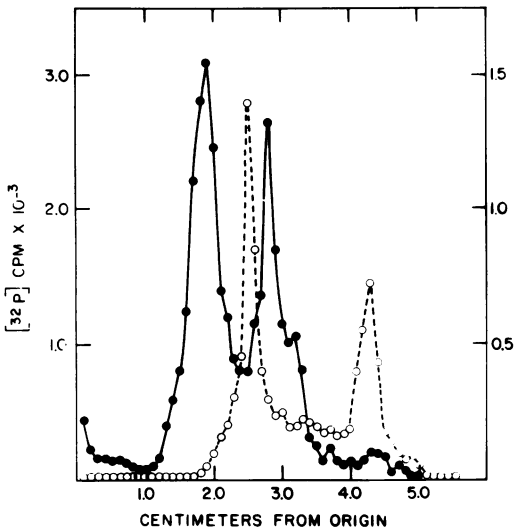

FIG. 2. *Agarose-acrylamide gel electrophoresis of ^{32}P-labeled FeSV(FeLV) RNA subunits in the presence of formamide (●). ^{3}H-labeled 28S and 18S rRNA's were co-electrophoresed in the same gel (○).*

after infection of mink cells with FeSV(FeLV) was electrophoretically separated, transferred to nitrocellulose, and hybridized with ^{32}P-labeled DNA transcripts prepared with an FeSV(FeLV) RNA template. Three major bands were identified (Fig. 3A, lane 1), corresponding to DNA molecules of 8.4, 6.7, and 5.0 kbp. To determine initially which of these forms represented unintegrated FeSV proviral DNA, the total FeSV(FeLV) cDNA was hybridized to RNA purified from pseudotype virions [FeSV(AT-124)] obtained from FeSV-transformed nonproducer rat cells infected with a heterologous murine helper virus. Such selected transcripts (FeSV $cDNA_{rep}$) contain sarcoma virus-specific sequences (designated *src*), as well as other sequences shared in common by FeSV and FeLV (designated *com*), but lack all sequences unique to the helper virus. When $cDNA_{rep}$ (Fig. 3A, lane 2) was used, the relative autoradiographic intensity of the 5.0-kbp band was increased, suggesting that the 5.0-kbp band was an FeSV proviral DNA form, whereas the 8.4- and 6.7-kbp bands did not contain FeSV-specific sequences.

In principle, the three bands could represent either linear or circular forms of FeSV(FeLV) extrachromosomal DNA. Figure 3A, lane 3 shows that *Eco*RI digestion reduced the lengths of each of the three DNA species by approximately 0.7 kbp. Although reciprocal *Eco*RI fragments of 0.7 kbp were not detected, two smaller *Eco*RI fragments of 0.4 and 0.3 kbp were seen in overexposed autoradiographs developed for 10 to 14 days (data not shown). These data are consistent with the interpretation that *Eco*RI cuts each of the DNA forms at sites near the termini of linear molecules.

To confirm that the 5.0-kbp band represented the linear FeSV provirus, the cellular DNA of FeSV-transformed nonproducer cells was analyzed for the presence of integrated FeSV DNA after *Eco*RI digestion. Each transformed clone was derived from an independent infectious event. Figure 3B shows representative results obtained with the cellular DNA of two such clones. When restricted, uninfected mink cell DNA was used, one prominent high-molecular-weight band was detected after hybridization with $cDNA_{rep}$ (Fig. 3B, lane 1). In contrast, the DNA of FeSV-transformed cells contained an additional 4.3-kbp band which was readily resolved after *Eco*RI digestion (Fig. 3B, lanes 2 and 3). These results showed (i) that the 5.0-kbp band found in extrachromosomal DNA preparations of cells acutely infected with FeSV(FeLV) represents linear FeSV DNA, and (ii) that *Eco*RI recognizes cleavage sites at each end of the DNA provirus (see below). As an additional control for these experiments, we showed that the enzyme *Hin*dIII, which fails to cleave 5.0-kbp FeSV DNA, generates bands (>5.0 kbp) containing both viral and host cell sequences after digestion of the DNA of nonproducer FeSV-transformed cells (manuscript in preparation).

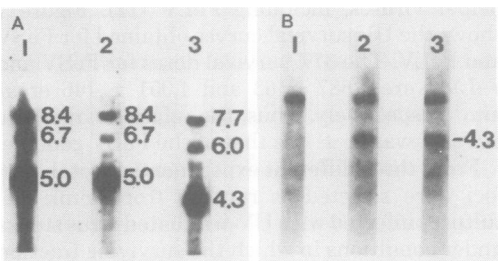

FIG. 3. *(A) Forms of unintegrated FeSV(FeLV) proviral DNA detected in mink cells 24 h after infection. Electrophoresis was performed in 1.0% agarose. Lane 1 shows undigested DNA forms detected with ^{32}P-labeled total FeSV(FeLV) cDNA. Lanes 2 and 3 show results obtained with ^{32}P-labeled FeSV $cDNA_{rep}$ either before (lane 2) or after (lane 3) digestion with EcoRI. The numbers to the right of the bands indicate the lengths of linear molecules in kilobase pairs. (B) Integrated FeSV DNA excised with EcoRI from the cellular DNA of mink cells nonproductively transformed with FeSV. Electrophoresis was performed in 0.8% agarose. Lane 1 shows uninfected mink DNA, and lanes 2 and 3 show results obtained with the DNA of two representative focus-derived clones obtained either by endpoint dilution or after UV irradiation. Hybridizations were performed with $cDNA_{rep}$.*

To define further the nature of extrachromosomal FeSV(FeLV) DNA molecules, the biological activities of the three classes of unintegrated DNA were studied in transfection experiments. The 8.4-, 6.7-, and 5.0-kbp bands were electroeluted from agarose, and the specific infectivities of these DNA preparations were compared with that of total FeSV(FeLV) extrachromosomal DNA. Uninfected mink Mv1Lu and cat CCC clone 81 cells served as recipient cultures to assay replicating helper virus activity. The transforming capacity of FeSV DNA was determined by focus formation in NIH/3T3 cells and in mink cells superinfected with replicating FeLV helper virus. The latter cells require the presence of replicating helper virus for transformation to be observed. Similar observations were made with Moloney murine sarcoma virus DNA cloned in bacteriophage lambda (D. Blair and G. F. Vande Woude, personal communication). Thus, the helper virus-dependent nature of sarcoma virus-induced transformation in mink cells is a property of the recipient cells and is not particular to FeSV proviral DNA.

Table 1 shows that the replicating helper virus activity detected in total extrachromosomal DNA resided in the 8.4-kbp DNA species, whereas the 5.0-kbp DNA molecules carried the FeSV-transforming capacity. The 6.7-kbp DNA preparation lacked detectable biological activity that could be identified in any of the assays. Although areas of typical ST-FeSV-transformed cells were observed in a few cell cultures inoculated with total FeSV(FeLV) DNA, these cells invariably produced replicating FeSV(FeLV) particles. Although transfection of mink cells with the 5.0-kbp DNA preparation did not lead to observed transformation, superinfection of recipient cultures with nontransforming FeLV led to the appearance of typical FeSV foci. Infectious transforming FeSV(FeLV) was detected in media from these cultures. In contrast, transformation of NIH/3T3 mouse cells with 5.0-kbp DNA did not require the presence of helper viral activity (22). FeSV DNA-transformed NIH/3T3 cells did not produce infectious virus but contained FeSV genomes which could be rescued with mouse type C helper virus. Thus, we conclude that the 8.4-kbp species represents the biologically active provirus of FeLV, whereas the 5.0-kbp species is an infectious FeSV DNA. Restriction mapping of the 8.4- and 6.7-kbp species shows that both forms are linear DNA molecules; the 6.7-kbp molecule is a deletional variant of the 8.4-kbp band (unpublished data) and is not discussed further.

Although unintegrated DNA forms obtained after 24 h of infection represented predominantly linear molecules, circular DNA forms could also be identified (18, 20, 31, 32, 46, 48).

TABLE 1. *Infectivity of ST-FeSV(FeLV) DNA*[a]

DNA preparation	Biological activity of DNA				
	Replicating FeLV production in:		FeSV transformation in:		
	CCC clone 81[b]	Mv1Lu[b]	Mv1Lu[b]	FeLV-infected Mv1Lu[b]	NIH/3T3[c]
Total extrachromosomal DNA	9.6	11.4	≤1.4[d]	22.3	4/6
8.4-kbp fraction	8.1	9.6	<0.15	<0.15	0/6
6.7-kbp fraction	<0.15	<0.15	<0.15	<0.15	0/6
5.0-kbp fraction	<0.15	≤0.15[e]	<0.15	5.7	2/6

[a] The infectivities of the various DNA preparations were tested in four recipient cell systems. Infectious units per microgram of DNA were calculated from the 50% infectious dose determined by endpoint dilution. DNA species 8.4, 6.7, and 5.0 kbp long were obtained by electroelution (23) and reconcentrated, and their purities were confirmed by the Southern transfer technique (39) using a ^{32}P-labeled total FeSV(FeLV) cDNA transcript. Individual autoradiographic bands were free of detectable DNA species of other apparent size classes.

[b] Values represent infectious units per microgram of DNA (1 50% infectious dose = 1 infectious unit). For fractionated DNA species, microgram values were standardized to the total DNA used for electroelution and do not represent the actual quantities of each DNA species recovered. As such, the values for infectious units per microgram represent the minimal estimate of specific infectivity.

[c] Number of FeSV-transformed focus-containing cultures per total number of cultures inoculated with 0.7 μg of DNA per well.

[d] One of three cultures inoculated with the highest DNA dose (7.0 μg/well) contained FeSV-transformed cell foci and produced infectious FeSV(FeLV).

[e] One of three cultures inoculated with the highest DNA dose (7.0 μg/well) produced replicating helper virus.

These forms were considerably more prominent in mink cells infected for 48 h. The circular FeSV intermediate (form I DNA) migrated approximately two times faster than the 5.0-kbp linear form, whereas the circular form of 8.4-kbp DNA migrated at a position corresponding to ~5.3 kbp. Treatment of these circular DNA species with *Eco*RI reduced their electrophoretic mobility and converted them to linear molecules 7.7 and 4.3 kbp long, respectively (data not shown). In DNA preparations obtained 24 h after infection, we estimate that such forms represent 10% or less of the total proviral DNA and rarely complicate the analysis of 5.0-kbp FeSV DNA (see below).

Restriction mapping of ST-FeSV proviral DNA. To determine the locations of endonuclease cleavage sites in the FeSV linear DNA provirus, the 5.0-kbp DNA was electroeluted from agarose and subjected to further detailed analyses. Figure 4, lane 1 shows the 5.0-kbp DNA obtained after electroelution, and Fig. 4, lane 2 shows results obtained after digestion with *Eco*RI. As expected from the data in Fig. 3, electroeluted 5.0-kbp FeSV DNA was reduced in size by 0.7 kbp after *Eco*RI treatment. Analysis of *Eco*RI cleavage sites was facilitated by concomitant digestion with three enzymes that make single, asymmetrical cuts in FeSV DNA. Digestion with either *Bgl*II (Fig. 4, lane 3), *Bam*HI (lane 5), or *Xho*I (lane 7) produced two fragments whose aggregate chain lengths equaled that of FeSV DNA. Codigestion experiments with *Eco*RI (Fig. 4, lanes 4, 6, and 8) showed that each of the two *Bgl*II, *Bam*HI, or *Xho*I fragments was reduced in size by 0.3 to 0.4 kbp after *Eco*RI digestion, confirming that the latter enzyme recognizes cleavage sites close to both termini of the FeSV provirus.

Orientation of *Bgl*II, *Bam*HI, and *Xho*I sites was also achieved by dual digestion analyses. Codigestion of FeSV DNA with *Xho*I and *Bgl*II produced a central fragment of 2.2 kbp and two terminal fragments of 1.5 and 1.3 kbp (Fig. 4, lane 9). Similarly, codigestion with *Bam*HI and *Bgl*II produced an internal 2.4-kbp fragment and two terminal fragments of ~1.3 kbp which were not resolved from one another in the experiment shown (Fig. 4, lane 10). As predicted, codigestion with *Bam*HI and *Xho*I left the major *Xho*I fragment intact but reduced the size of the *Xho*I 1.5-kbp fragment to 1.3 kbp (Fig. 4, lane 11). These results positioned the *Bam*HI cleavage site outside the *Xho*I site on the same end of the linear provirus and showed that *Bgl*II cleaves at the opposite end of FeSV DNA from either *Bam*HI or *Xho*I.

Localization of cleavage sites for several other enzymes was achieved by similar experiments. The positions of these and previously discussed sites are summarized in Fig. 5. *Sal*I produced a single cut in FeSV DNA near the center of the genome at ~2.5 kbp. Codigestion with *Xho*I and *Sal*I yielded three fragments and showed that *Sal*I cleaves the major *Xho*I fragment (3.5 kbp) to two fragments of 0.95 and 2.55 kbp. This positioned the *Sal*I site at 0.95 kbp to the left of the *Xho*I site at ~2.55 kbp on the map. Codigestion with *Sal*I and *Bgl*II produced three fragments, reducing the major *Bgl*II fragment (3.7 kbp) to two fragments of 2.45 and 1.25 kbp. This independently positioned the *Sal*I site at 1.25 kbp to the right of the *Bgl*II site at the same map position (Fig. 5). As expected, *Eco*RI re-

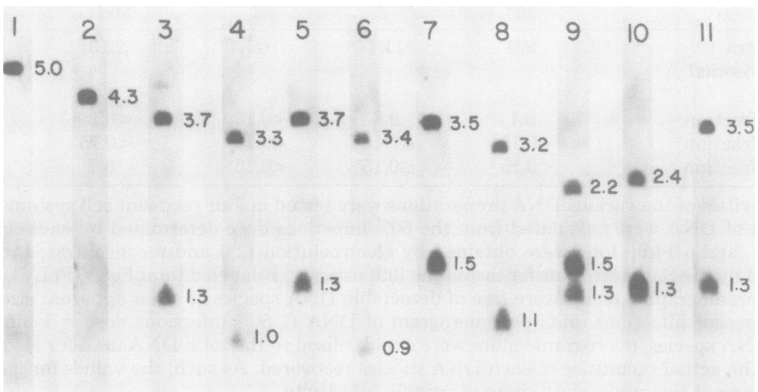

FIG. 4. *Digestion of 5.0-kbp FeSV proviral DNA with various restriction endonucleases. Hybridization reactions were performed by using ^{32}P-labeled cDNA$_{rep}$. The numbers to the right of the bands indicate the lengths of linear molecules in kilobase pairs. Lane 1, Unrestricted DNA obtained by electroelution; lane 2, EcoRI; lane 3, BglII; lane 4, BglII and EcoRI; lane 5, BamHI; lane 6, BamHI and EcoRI; lane 7, XhoI; lane 8, XhoI and EcoRI; lane 9, XhoI and BglII; lane 10, BamHI and BglII; lane 11, BamHI and XhoI.*

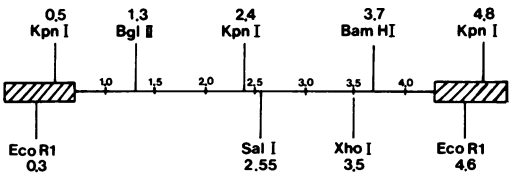

FIG. 5. *Restriction endonuclease map of 5.0-kbp FeSV linear proviral DNA. The cross-hatched squares at the termini indicate the extents of putative ETR sequences. Calibration is in kilobase pairs in the order 5' to 3' with respect to viral RNA.*

duced both *Sal*I fragments by 0.3 to 0.4 kbp.

*Kpn*I digestion yielded two major fragments (2.4 and 1.9 kbp), the sum of which was 0.7 kbp less than the size of full-length linear FeSV DNA. This suggested that *Kpn*I, like *Eco*RI, cut within terminal sequences at both ends of FeSV DNA but also cleaved at another, internal site. *Bgl*II digested the 1.9-kbp *Kpn*I fragment to two fragments of 1.1 and 0.8 kbp, and *Bam*HI cleaved the 2.4-kbp *Kpn*I fragment to two fragments of 1.3 and 1.1 kbp. Taken together, these results localized the internal *Kpn*I site at 1.1 kbp to the right of the *Bgl*II site and at 1.3 kbp to the left of the *Bam*HI site at 2.4 kbp on the map. These data also showed that *Kpn*I sites near the termini were located at 0.8 kbp to the left of the *Bgl*II site and at 1.1 kbp to the right of the *Bam*HI site. Confirmation of the asymmetry of *Kpn*I sites within the terminal sequences was obtained by codigestion experiments performed with *Eco*RI. As expected, the 1.9-kbp *Kpn*I fragment was resistant to *Eco*RI cleavage, and the 2.4-kbp *Kpn*I fragment was shortened by 0.2 kbp after *Eco*RI digestion.

The positions of *Kpn*I sites within the terminal sequences were further studied by codigestion analyses performed with purified terminal fragments generated by either *Bgl*II or *Xho*I. The left-hand 1.3-kbp *Bgl*II fragment and the right-hand *Xho*I fragment were purified by electroelution and digested with *Kpn*I, and the products were separated in 1.6% agarose gels. The small fragments were then covalently transferred to diazobenzyloxymethyl filter paper, which effectively immobilizes them and renders them susceptible to detection with ^{32}P-labeled cDNA transcripts (Alwine et al., in press). The 1.3-kbp *Bgl*II fragment was cleaved to two fragments of 0.8 and 0.5 kbp, whereas the 1.5-kbp *Xho*I fragment was shortened to 1.3 kbp after *Kpn*I digestion. These experiments confirmed that *Kpn*I recognizes cleavage sites at both ends of linear FeSV DNA molecules and localized the terminal sites as indicated in Figure 5. Further analyses of the specific sequences contained in the various restriction fragments are summarized below.

Position of the *src* sequence. ^{32}P-labeled cDNA transcripts complementary to either the *src* or *com* sequences of FeSV were prepared and hybridized to restriction fragments of FeSV proviral DNA in order to define the topological orientation of each subset of sequences. Fragments containing only *src* sequences would be expected to hybridize only to cDNA *src*, and fragments containing *com* sequences would be expected to hybridize only to cDNA *com*. Junctional fragments containing both *src* and *com* sequences would be expected to anneal with both cDNA species. In principle, the relative intensity of a junction fragment band using each cDNA would be a function of the relative complexity of *src* versus *com* sequences in that fragment since the specific activities of both cDNA's were the same and the relative amounts of each ^{32}P-labeled probe used in the hybridization reactions were approximately equal (see above). Autoradiographs obtained with $cDNA_{com}$ and $cDNA_{src}$ were analyzed on a scanning densitometer, and the tracings obtained with each specific, labeled transcript were superimposed. Figure 6 shows representative densitometric tracings plotted in arbitrary optical density units versus relative mobility. The sizes of fragments in kilobase pairs are indicated by numbers over each peak and correspond to the lengths of fragments expected from the map shown in Figure 5.

Figure 6A shows results obtained in a representative experiment with *Bgl*II and *Xho*I. Three bands were visualized, corresponding to the 1.5- and 1.3-kbp terminal fragments and the large 2.2-kbp internal fragment. The terminal fragments were detected only with $cDNA_{com}$, whereas the internal fragment was detected preferentially with $cDNA_{src}$. Consistent results were obtained in single-digestion analyses performed with either *Bgl*II, *Xho*I, or *Bam*HI. The 1.3-kbp *Bgl*II, 1.5-kbp *Xho*I, and 1.3-kbp *Bam*HI fragments could not be visualized with $cDNA_{src}$, whereas all were readily detected with $cDNA_{com}$. In control experiments, filter papers initially hybridized with $cDNA_{src}$ were exposed to 50% formamide–0.1× SSC at 75°C to remove labeled transcripts, and the papers were rehybridized with $cDNA_{com}$. The small terminal *Bgl*II, *Xho*I, and *Bam*HI fragments were again easily detected, confirming that the inability to visualize them with $cDNA_{src}$ was not due to inefficient transfer of these fragments to the solid support medium. These experiments positioned all *src* sequences between 1.3 and 3.5 kbp on the FeSV map (Fig. 5) and showed that *src* sequences were flanked by *com* sequences at each of the termini.

To study the distribution of *src* sequences within the center of FeSV DNA, codigestion

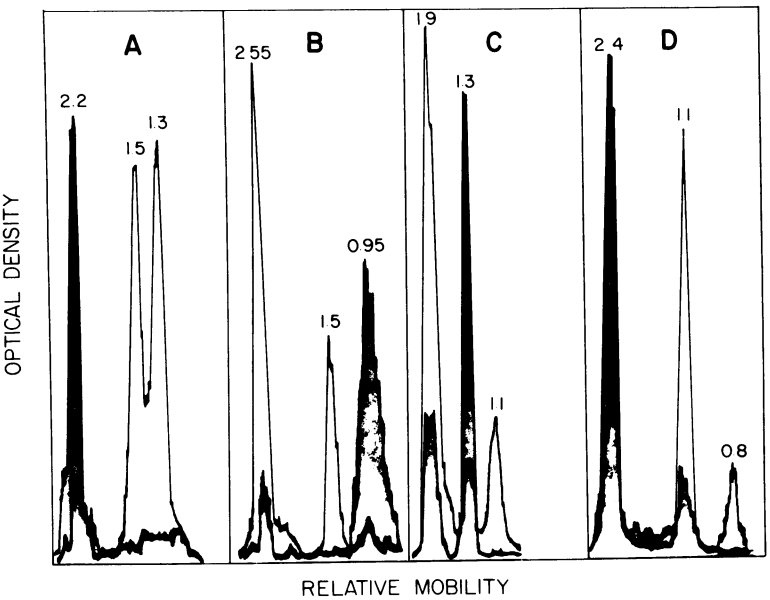

FIG. 6. *Codigestion of 5.0-kbp FeSV proviral DNA with various endonucleases. Each digestion was performed in duplicate and run in parallel lanes on the same gel. After transfer to nitrocellulose, the immobilized DNA fragments were annealed with either ^{32}P-labeled cDNA$_{src}$ (shaded areas) or cDNA$_{com}$ (open areas) of the same specific activity. Autoradiographs were developed, cut into strips, and scanned at 590 nm with a Gilford densitometer. The scan rate and recorder speed were both adjusted to 1 cm/min; the maximal absorbance was set to give ~100% deflection of the recorder pen for the most intense band. Curves were superimposed to produce the composite figure shown. The enzymes used were BglII and XhoI (A), SalI and XhoI (B), KpnI and BamHI (C), and KpnI and BglII (D). Numbers above peaks indicate the fragment lengths in kilobase pairs.*

experiments were performed with *Xho*I and *Sal*I (Fig. 6B). The internal 0.95-kbp fragment and terminal 2.55-kbp fragment were detected with both cDNA's, whereas the terminal 1.5-kbp *Xho*I fragment was again visualized only with cDNA$_{com}$. An analysis of band intensities showed that the majority of *src* sequences map within the 0.95-kbp fragment, whereas the 2.55-kbp fragment hybridized with far greater efficiency to cDNA$_{com}$. Thus, *src* sequences were localized to a region beginning at the left of the *Sal*I site and extending close to the *Xho*I site, within 3.5 kbp on the map (Fig. 5).

The left-hand limit of the *src* sequence (Fig. 5) was further defined by codigestion experiments performed with *Kpn*I and *Bam*HI (Fig. 6C) or with *Kpn*I and *Bgl*II (Fig. 6D). As expected, the internal 1.3-kbp fragment generated by *Bam*HI and *Kpn*I hybridized preferentially to cDNA$_{src}$; *src* sequences extended to the left of the *Kpn*I site into the 1.9-kbp fragment. Codigestion with *Bgl*II and *Kpn*I confirmed that *src* sequences extended into the 1.1-kbp junctional fragment defined by these enzymes and directly showed that the region between 1.3 and 2.4 kbp on the map contained considerably more *com* than *src* sequences.

Although the complexity of *src* sequences could not be determined precisely by these methods, the limits of these sequences were estimated by quantitative densitometric measurements. Table 2 summarizes data from three experiments performed with different extrachromosomal DNA preparations and with independently synthesized *src* probes. To compare densitometric peaks from different experiments, the recorded intensities were normalized and averaged (standard deviation for all determinations, less than ±8%). Intensities were then corrected for fragment length. By using *Sal*I and *Xho*I, ~90% of the *src* sequences were detected within the 0.95-kbp internal fragment, whereas only 10% were found to the left of the *Sal*I site. Thus, the maximal complexity of *src* sequences within the large *Sal*I terminal fragment should be less than 10% of 0.95 kbp, or ~0.1 kbp. Similarly, codigestion experiments performed with *Kpn*I and *Bam*HI limited the extent of *src* sequences to the left of the *Kpn*I site to less than 20% of 1.3 kbp, or a maximum of 0.26 kbp. The differences observed in measurements obtained with different enzymes are within the range of experimental error and also reflect the fact that the 1.3-kbp *Kpn*I-*Bam*HI fragment contains some-

TABLE 2. *Relative labeling of FeSV restriction fragments with cDNA$_{src}$*

Enzymes used	Size of fragment (kbp)	Map position[a] (kbp)	Avg intensity (mg%)[b]	Relative intensity (mg% per kbp)[c]
*Bgl*II and *Xho*I	2.2	1.3–3.5	97	44
	1.5	3.5–5.0	<1.5	<1.0
	1.3	0.0–1.3	<1.5	<1.2
*Sal*I and *Xho*I	2.55	0.0–2.55	24	9.4
	1.5	3.5–5.0	<2.0	<1.4
	0.95	2.55–3.5	74	78
*Bam*HI and *Kpn*I	1.9	0.5–2.4	24	13
	1.3	2.4–3.7	74	57
	1.1	3.7–4.8	<1.8	<1.7
*Bgl*II and *Kpn*I	2.4	2.4–4.8	83	35
	1.1	1.3–2.4	15	14
	0.8	0.5–1.3	<2.5	<2.8

[a] Positions correspond to those shown in the map in Fig. 5.

[b] Areas under densitometric peaks were determined by weight measurement (milligrams). Data for three experiments were normalized to a total intensity of 100, and the average intensity (standard deviation, ±8%) for each band was computed.

[c] Average intensities for each fragment were divided by the length of the fragment in kilobase pairs. When transcripts representative of the entire FeSV genome were used, the intensities of bands in a single lane were principally a function of fragment size (see text). The relative intensities are therefore an index of the relative distribution of *src* sequences between different fragments.

what more *com* sequences than the 0.95-kbp *Sal*I-*Xho*I fragment (Fig. 6). We estimate, then, that the maximal complexity of *src* sequences in FeSV DNA is ~1.3 kbp and that these sequences are localized between 2.1 and 3.4 kbp on the map (Fig. 5).

Orientation of 3′ and 5′ ends. In several retroviral systems, linear unintegrated proviral DNAs have been found to be from 0.3 to 1.2 kbp longer than their respective viral RNA genomes (3, 8, 18, 29, 31, 32). Both termini of proviral DNA are now known to contain extended terminal redundancies (ETR sequences), each composed of sequences derived from both the 3′ and 5′ ends of viral RNA (18, 32; E. Gilboa, S. Goff, A. Shields, F. Yoshimura, S. Mitra, and D. Baltimore, Cell, in press). The orientation of sequences within the retroviral DNAs studied to date is 3′5′—3′5′, where the line designates non-ETR regions containing the viral structural genes (18, 32). The data presented above show that the FeSV provirus is ~0.7 kbp longer than FeSV RNA and contains *Eco*RI and *Kpn*I restriction sites near both termini. Digestion with each of these enzymes reduces the length of 5.0-kbp DNA by an aggregate 0.7 kbp. This is consistent with the possibility that the FeSV provirus contains ETR sequences ~0.7 kbp long. If this were the case, DNA transcripts complementary to either the 3′ or the 5′ end of viral RNA would be expected to hybridize to both ends of proviral DNA.

The presence of 5′-derived sequences at each terminus of FeSV DNA was established by using transcripts complementary to the extreme 5′ end of viral RNA. Such transcripts were prepared by using 60S FeSV(FeLV) RNA as the template and no exogenous primer. The products of these reactions included an ~140-base strong stop cDNA species (17), which was purified by polyacrylamide gel electrophoresis and recovered. Table 3 shows the results obtained when cDNA$_{5'}$ was hybridized to various FeSV DNA restriction fragments and compares these results with results obtained with cDNA$_{rep}$. When transcripts representing the entire FeSV genome were used, the intensities of bands corresponding to different restriction fragments were primarily a function of fragment length. In contrast, cDNA$_{5'}$ hybridized preferentially to terminal DNA fragments derived from both ends of FeSV DNA. Digestion with *Bgl*II or *Xho*I showed that both terminal fragments were readily detected, whereas the internal fragment generated by codigestion with both of these enzymes was very poorly visualized.

FeSV DNA was oriented with respect to viral RNA by codigestion experiments performed by using either *Bgl*II and *Eco*RI or *Bam*HI and *Eco*RI. *Eco*RI removes sequences of 0.3 to 0.4 kbp from each end of linear FeSV molecules;

TABLE 3. *Orientation of the 5′ end of linear FeSV DNA with respect to viral RNA*

Restriction enzyme(s) used	Size of fragment (kbp)	Map location[a] (kbp)	Avg intensity (mg%)[b]	
			cDNA$_{rep}$	cDNA$_{5'}$
*Bgl*II	3.7	1.3–5.0	77	56
	1.3	0.0–1.3	23	44
*Xho*I	3.5	0.0–3.5	75	54
	1.5	3.5–5.0	25	46
*Bgl*II and *Xho*I	2.2	1.3–3.5	52	5
	1.5	3.5–5.0	27	49
	1.3	0.0–1.3	21	46
*Bgl*II and *Eco*RI	3.3	1.3–4.6	76	8
	1.0	0.3–1.3	24	92
*Bam*HI and *Eco*RI	3.4	0.3–3.7	82	90
	0.9	3.7–4.6	18	10

[a] Position of fragments as indicated on the map in Fig. 5.

[b] Areas under densitometric peaks determined by weight measurement were summed and normalized to a total intensity of 100. The percentage of the total intensity recorded for each fragment was then calculated.

assuming that the order of sequences in each ETR region is 3'5', *Eco*RI would be expected to remove 3'-derived sequences from one terminus and all 5'-derived sequences from the other end of FeSV DNA. This would generate DNA molecules containing 5'-derived sequences only at the terminus corresponding to the 5' end of viral RNA. Table 3 shows that the small *Bgl*II-*Eco*RI and large *Bam*HI-*Eco*RI fragments were preferentially detected with $cDNA_{5'}$. Thus, *Bgl*II recognizes a cleavage site closer to the 5'-derived end of FeSV DNA, orienting the map shown in Fig. 5 from 5' to 3' with respect to viral RNA.

We also attempted to orient FeSV DNA by using $cDNA_{3'}$ transcripts prepared with a 12S to 18S poly(A)-containing FeSV(FeLV) template and calf thymus primer. Such transcripts were assumed to contain 3'-derived sequences of FeSV RNA which are not included in the ETR regions and were therefore expected to hybridize with greater efficiency to DNA fragments representing the 3' end of viral RNA. Sequences derived from the 3' end of FeSV(FeLV) RNA were detected at both termini of FeSV DNA; however, $cDNA_{3'}$ transcripts hybridized with relatively equal efficiency to the small *Bam*HI and *Bgl*II terminal fragments (data not shown). The interpretation of these results is that the $cDNA_{3'}$ transcripts copied from a template containing a fivefold molar excess of FeLV RNA (see above) annealed preferentially only to sequences within the ETR regions of FeSV DNA. Recent studies performed with FeSV and FeLV DNA cloned in bacteriophage λ indeed show that the ETR sequences of FeLV and FeSV are homologous. In contrast, non-ETR sequences to the right of the FeSV *Xho*I site are derived from an internal FeLV sequence localized approximately 2.0 to 2.5 kilobases from the 3' end of FeLV RNA which was not represented in $cDNA_{3'}$ transcripts. R-looping experiments performed with poly(A)-containing FeSV RNA have confirmed the orientation reported here when $cDNA_{5'}$ was used (C. J. Sherr, L. A. Fedele, M. Sullivan, M. Oskarrson, and G. F. Vande Woude, Cold Spring Harbor Conference on Cell Proliferation, VII, in press).

DISCUSSION

An analysis of extrachromosomal DNA from cells acutely infected with ST-FeSV(FeLV) defined three major species of unintegrated proviral DNA. Several lines of evidence show that the 5.0-kbp DNA form corresponds to the linear FeSV provirus, whereas the 8.4-kbp form represents the provirus of FeLV. A comparison of the relative target sizes of FeSV and FeLV genomes indicated that FeSV was slightly more than one-half the size of FeLV, which is in good agreement with direct length measurements performed with ^{32}P-labeled FeSV(FeLV) RNA. In addition, cDNA transcripts representing sequences unique to FeSV hybridized only with the 5.0-kbp DNA band, indicating that it alone contained sarcoma-specific sequences. Transfection experiments confirmed that the 5.0-kbp band can induce helper virus-independent foci in FeSV-transformed NIH/3T3 mouse cells and helper virus-dependent foci in Mv1Lu mink cells, whereas the 8.4-kbp DNA gives rise to nontransforming, replicating virus when inoculated into either mink or cat cells. Finally, *Eco*RI, which recognizes sites at both termini of the FeSV provirus and generates an internal 4.3-kbp fragment, was shown to excise integrated FeSV proviral DNA of corresponding length from the DNA of transformed nonproducer cells.

Measurements of the FeSV genome size suggest that the RNA genome is ~0.7 kbp shorter than linear proviral DNA. Sequences homologous to both the 5' and 3' ends of viral RNA were detected at both termini of FeSV DNA. Moreover, two enzymes were shown to recognize cleavage sites at both termini, reducing the length of the linear provirus by an aggregate 700 bases. Thus, like other type C proviruses (18, 32; Gilboa et al., in press), FeSV viral genes appear to be flanked by ETR sequences. Our data also suggest that the FeLV provirus (8.4 kbp) and an FeLV deletional variant (6.7 kbp) contain the same ETR sequences as those found in FeSV, indicating that these are derived from the natural helper virus.

Hybridization reactions performed with FeSV $cDNA_{src}$ and $cDNA_{com}$ showed that the FeSV *src* sequence is localized in the middle of FeSV proviral DNA and is flanked at both ends by sequences derived from the helper virus; *src* sequences were estimated to be 1.3 kbp long and were positioned between 2.1 and 3.4 kbp on the FeSV map. These data represent our best approximation of the complexity of *src* sequences since the analysis is limited by the number and distribution of mapped restriction enzyme cleavage sites and by the efficiency of nucleic acid hybridization techniques in defining junctional fragments containing both *src* and *com* elements.

Different strains of FeSV code for at least one polyprotein containing both *gag* and FOCMA-S antigenic determinants (27, 34, 40). In the ST strain, this protein has an apparent molecular weight of 78,000 and contains N-terminal p15 and p12, but not p30, antigens (S. Ruscetti, L. P. Turek, and C. J. Sherr, unpublished data); larger polyproteins are found in the Gardner-Arnstein and McDonough strains of FeSV, the latter of which contains p30 antigenic determinants (27,

34, 40). The C-terminal portion of the ST-FeSV polyprotein which contains the FOCMA-S moiety would, then, be expected to have an apparent molecular weight of ~50,000. FOCMA-S does not react with antisera directed against any of the known FeLV structural proteins (34, 35, 40), suggesting that this portion of the polyprotein could be encoded by *src* sequences.

Assuming that ETR sequences do not code for *gag* gene products, we would estimate that sequences coding for p15 and p12 extend to at least 1.5 kbp from the 5′ end of the FeSV provirus. In the Moloney murine sarcoma virus, ETR sequences of similar lengths have been demonstrated by several techniques (Gilboa et al., in press; G. F. Vande Woude, M. Oskarsson, L. W. Enquist, S. Nomura, M. Sullivan, and P. J. Fischinger, Proc. Natl. Acad. Sci. U.S.A., in press), and sequences coding for p15 and p12 have been assigned to within 2.0 kbp of the 5′ end of Moloney murine sarcoma virus linear DNA (Vande Woude et al., in press). The data presented here show that *com* sequences terminate at approximately 2.1 kbp from the 5′ end of FeSV linear DNA, which is consistent with the interpretation that these code for *gag* gene p15 and p12 antigens. In several oncornaviral systems, "*gag*-X" polyproteins have been identified, which are analogous to the polyprotein product of FeSV (6, 19, 25, 47). Cell-free translation of the RNA genomes of these viruses indicates that the *gag*-X polyproteins can be synthesized in vitro by using full-length viral RNA as the message (25, 47). Thus, the gene(s) coding for the X portions of these proteins are contiguous with *gag* sequences in viral RNA. In the FeSV system, cell-free translation of FeSV(FeLV) RNA also generates a 78,000-dalton product which is precipitable with antisera to *gag* antigens (S. Ruscetti, R. Callahan, and C. J. Sherr, unpublished data). Thus, if the sequences encoding *gag* and X are contiguous in FeSV RNA as well, we would expect that sequences encoding X would extend from approximately 2.0 kbp to 3.4 kbp on the FeSV map, a region corresponding to *src* sequences. Our data do not show, however, that X is the only *src* gene product, since we cannot exclude the possibility that a limited region of the *src* sequence encodes an additional small polypeptide. It is also unclear whether the *com* sequences to the right of the *Xho*I site can code for other proteins as well.

If the *src* gene indeed encodes FOCMA-S, one clear prediction of our studies would be that the FOCMA antigens of the ST and McDonough strains of FeSV would be antigenically distinct, since each of these viruses contains a different *src* sequence (13). Preliminary experiments with defined rabbit antisera raised to FOCMA-containing FeSV pseudotype virions (35) support this conclusion (S. Ruscetti, L. P. Turek, and C. J. Sherr, unpublished data). Additional evidence in favor of an association of viral transformation and FOCMA expression comes from studies of ST-FeSV-transformed, nonproducer mink cell clones derived from extensively UV-irradiated viral stocks, all of which have been found to express the *gag*-X polyprotein (manuscript in preparation). The determination of whether this product is directly responsible for FeSV-induced transformation must await the more precise localization of the exact gene sequences required for focus formation. Transfection experiments performed with defined restriction fragments of FeSV DNA could facilitate a more direct analysis and would potentially define the minimal genetic information required for both transformation and FOCMA expression in vitro (1).

Lymphoid tumor cells induced by FeLV alone have also been reported to express FOCMA, as defined by immunofluorescence criteria (11). Since the nature of FOCMA in these cells has not been chemically determined, we have designated the antigen induced by FeLV as FOCMA-L and that induced by FeSV as FOCMA-S (35). The endogenous nature of *src*-related genes in normal cat DNA (13) suggests that FOCMA-L expression could reflect transcription of endogenous *src* sequences. Alternatively, the apparent cross-reactions observed between FOCMA-L and FOCMA-S may reflect the fortuitously similar titers of two different antibody populations in the sera used to detect these molecules.

An understanding of the organization of FeSV genomes makes it possible to clone defined viral genes in procaryotic vectors and to readily obtain DNA molecules representing subgenomic fragments. Recent data indicate that *Eco*RI-digested linear DNA intermediates of both ST-FeSV and FeLV can be cloned in suitable bacteriophage λ vectors with high efficiency (C. J. Sherr et al., in press). Such reagents should be useful in defining the organization of FeLV-related endogenous viral genes in the normal cat cellular genome, in characterizing the topology of endogenous *src*-related genes, and in determining the roles of each of these elements in naturally occurring malignancies of cats.

ACKNOWLEDGMENTS

We thank Dominique Stehelin, Martine Roussel, Michael Bishop, and G. Steven Martin for providing protocols and sharing the results of unpublished data with us, James Alwine for supplying and helping us prepare activated filter paper to covalently conjugate small DNA fragments, George Khoury for the use of his photographic facilities, and George Vande Woude, Peter Fischinger, Shigeko Nomura, and Sandra Rus-

cetti for helpful discussions throughout the progress of this work. We also appreciate the able technical assistance of John Kvedar and Thomas Shaffer, who helped with these experiments, and Doris Little, who typed the manuscript.

This work was supported in part by the Virus Oncology Program of the National Cancer Institute.

LITERATURE CITED

1. **Andersson, P., M. P. Goldfarb, and R. A. Weinberg.** 1979. A defined subgenomic fragment of *in vitro* synthesized Moloney sarcoma virus DNA can induce cell transformation upon transfection. Cell **16**:63–75.
2. **Ando, T.** 1966. A nuclease specific for heat-denatured DNA isolated from a product of *Aspergillus oryzae*. Biochim. Biophys. Acta **114**:158–168.
3. **Baltimore, D., E. Gilboa, E. Rothenberg, and F. Yoshimura.** 1978. Production of a discrete infectious, double-stranded DNA by reverse transcription in virions of Moloney murine leukemia virus. Cold Spring Harbor Symp. Quant. Biol. **43**:869–874.
4. **Benveniste, R. E., R. Heinemann, G. L. Wilson, R. Callahan, and G. J. Todaro.** 1974. Detection of baboon type C viral sequences in various primate tissues by molecular hybridization. J. Virol. **14**:56–67.
5. **Benveniste, R. E., C. J. Sherr, and G. J. Todaro.** 1975. Evolution of type C viral genes: origin of feline leukemia virus. Science **190**:886–888.
6. **Bister, K., M. J. Hayman, and P. K. Vogt.** 1977. Defectiveness of avian myelocytomatosis virus MC29: isolation of long-term nonproducer cultures and analysis of virus-specific polypeptide synthesis. Virology **82**:431–448.
7. **Britten, R. J., and D. E. Kohne.** 1968. Repeated sequences in DNA. Science **161**:529–540.
8. **Canaani, E., P. Duesberg, and D. Dina.** 1977. Cleavage map of linear mouse sarcoma virus DNA. Proc. Natl. Acad. Sci. U.S.A. **74**:24–33.
9. **Cooper, G. M., and H. M. Temin.** 1974. Infectious Rous sarcoma virus and reticuloendotheliosis virus DNAs. J. Virol. **14**:1132–1141.
10. **Copeland, N. G., and G. M. Cooper.** 1979. Transfection by exogenous and endogenous murine retrovirus DNAs. Cell **16**:347–356.
11. **Essex, M.** 1975. Horizontally and vertically transmitted oncornaviruses of cats. Adv. Cancer Res. **21**:175–248.
12. **Fischinger, P. J., C. S. Blevins, and S. Normura.** 1974. Simple, quantitative assay for both xenotropic murine leukemia and ecotropic feline leukemia viruses. J. Virol. **14**:177–179.
13. **Frankel, A. E., J. H. Gilbert, K. J. Porzig, E. M. Scolnick, and S. A. Aaronson.** 1979. Nature and distribution of feline sarcoma virus nucleotide sequences. J. Virol. **30**:821–827.
14. **Friis, R. R.** 1971. Inactivation of avian sarcoma viruses with UV light: a difference between helper-dependent and helper-independent strains. Virology **43**:521–523.
15. **Gardner, M. B., R. W. Rongey, P. Arnstein, J. D. Estes, P. Sarma, R. J. Huebner, and C. G. Rickard.** 1970. Experimental transmission of feline fibrosarcoma to cats and dogs. Nature (London) **226**:807–809.
16. **Graham, F. L., and A. J. van der Eb.** 1973. Transformation of rat cells by DNA of human adenovirus 5. Virology **54**:536–539.
17. **Haseltine, W. A., D. G. Kleid, A. Panet, E. Rothenberg, and D. Baltimore.** 1976. Ordered transcription of RNA tumor virus genomes. J. Mol. Biol. **106**:109–131.
18. **Hsu, T. W., J. L. Sabran, G. E. Mark, R. V. Guntaka, and J. M. Taylor.** 1978. Analysis of unintegrated avian RNA tumor virus double-stranded DNA intermediates. J. Virol. **28**:810–818.
19. **Hu, S. S. F., C. Moscovici, and P. K. Vogt.** 1978. The defectiveness of Mill Hill 2, a carcinoma-inducing avian oncovirus. Virology **89**:162–178.
20. **Hughes, S. H., P. R. Shank, D. H. Spector, H. J. Kung, J. M. Bishop, H. E. Varmus, P. K. Vogt, and M. L. Breitman.** 1978. Proviruses of avian sarcoma virus are terminally redundant, coextensive with unintegrated linear DNA and integrated at many sites. Cell **15**:1397–1410.
21. **Khan, A., and J. R. Stephenson.** 1977. Feline leukemia virus: biochemical and immunological characterization of *gag* gene-coded structural proteins. J. Virol. **23**:599–607.
22. **Lowy, D., E. Rands, and E. M. Scolnick.** 1978. Helper-independent transformation by unintegrated Harvey sarcoma virus DNA. J. Virol. **26**:291–298.
23. **McDonell, M. W., N. Simon, and F. W. Studier.** 1977. Analysis of restriction fragments of T7 DNA and determination of molecular weights by electrophoresis in neutral and alkaline gels. J. Mol. Biol. **110**:119–146.
24. **McDonough, S. K., S. Larsen, R. S. Brodey, N. D. Stock, and W. D. Hardy.** 1971. A transmissible feline fibrosarcoma of viral origin. Cancer Res. **31**:953–956.
25. **Mellon, P., A. Pawson, K. Bister, G. S. Martin, and P. H. Duesberg.** 1978. Specific RNA sequences and gene products of MC29 avian acute leukemia virus. Proc. Natl. Acad. Sci. U.S.A. **75**:5874–5878.
26. **Nomura, S., R. H. Bassin, W. Turner, D. K. Haapala, and P. J. Fischinger.** 1972. Ultraviolet inactivation of Moloney leukaemia virus: relative target size required for virus replication and rescue of "defective" murine sarcoma virus. J. Gen. Virol. **14**:213–217.
27. **Porzig, K. J., M. Barbacid, and S. A. Aaronson.** 1979. Biological properties and translational products of three independent isolates of feline sarcoma virus. Virology **92**:91–107.
28. **Reed, L. J., and H. Muench.** 1938. A simple method of estimating fifty per cent endpoints. Am. J. Hyg. **27**:212–215.
29. **Rothenberg, E., D. Smotkin, D. Baltimore, and R. A. Weinberg.** 1977. *In vitro* synthesis of infectious DNA of murine leukemia virus. Nature (London) **269**:122–126.
30. **Sen, A., C. J. Sherr, and G. J. Todaro.** 1976. Specific binding of the type C viral core protein p12 with purified viral RNA. Cell **7**:21–32.
31. **Shank, P. R., J. C. Cohen, H. E. Varmus, K. Yamamoto, and G. M. Ringold.** 1978. Mapping of linear and circular forms of mouse mammary tumor virus DNA with restriction endonucleases: evidence for a large specific deletion occurring at high frequency during circularization. Proc. Natl. Acad. Sci. U.S.A. **75**:2112–2116.
32. **Shank, P. R., S. H. Hughes, H.-J. Kung, J. E. Majors, N. Qunitrell, R. V. Guntaka, J. M. Bishop, and H. E. Varmus.** 1978. Mapping unintegrated avian sarcoma virus DNA: termini of linear DNA bear 300 nucleotides present once or twice in two species of circular DNA. Cell **15**:1383–1395.
33. **Sherr, C. J., R. E. Benveniste, and G. J. Todaro.** 1978. Endogenous mink (*Mustela vison*) type C virus isolated from sarcoma virus-transformed mink cells. J. Virol. **25**: 738–749.
34. **Sherr, C. J., A. Sen, G. J. Todaro, A. Sliski, and M. Essex.** 1978. Pseudotypes of feline sarcoma virus contain an 85,000 dalton protein with feline oncornavirus-associated cell membrane antigen (FOCMA) activity. Proc. Natl. Acad. Sci. U.S.A. **75**:1505–1509.
35. **Sherr, C. J., G. J. Todaro, A. Sliski, and M. Essex.** 1978. Characterization of a feline sarcoma virus-coded antigen (FOCMA-S) by radioimmunoassay. Proc. Natl. Acad. Sci. U.S.A. **75**:4489–4493.
36. **Shoyab, M., and A. Sen.** 1978. A rapid method for the purification of extrachromosomal DNA from eukaryotic

cells. J. Biol. Chem. **253**:6654–6656.

37. **Sliski, A., M. Essex, C. Meyer, and G. J. Todaro.** 1977. Feline oncornavirus-associated cell membrane antigen: expression in transformed nonproducer mink cells. Science **196**:1336–1338.
38. **Snyder, S. P., and G. H. Theilen.** 1969. Transmissible feline fibrosarcoma. Nature (London) **221**:1074–1075.
39. **Southern, E. M.** 1975. Detection of specific sequences among DNA fragments separated by gel electrophoresis. J. Mol. Biol. **98**:503–517.
40. **Stephenson, J. R., A. S. Khan, A. H. Sliski, and M. Essex.** 1977. Feline oncornavirus-associated cell membrane antigen: evidence for an immunologically cross-reactive feline sarcoma virus-coded protein. Proc. Natl. Acad. Sci. U.S.A. **74**:5608–5612.
41. **Stow, N. D., and N. M. Wilkie.** 1976. An improved technique for obtaining enhanced infectivity with herpes virus type 1 DNA. J. Gen. Virol. **33**:447–458.
42. **Todaro, G. J., P. Arnstein, W. P. Parks, E. H. Lennette, and R. J. Huebner.** 1973. A type C virus in human rhabdomyosarcoma cells after inoculation into anti-thymocyte serum-treated NIH Swiss mice. Proc. Natl. Acad. Sci. U.S.A. **70**:859–862.
43. **Toyoshima, K., and P. K. Vogt.** 1969. Enhancement and inhibition of avian sarcoma viruses by polycations and polyanions. Virology **38**:414–426.
44. **Tronick, S. R., C. D. Cabradilla, S. A. Aaronson, and W. A. Haseltine.** 1978. 5′-Terminal nucleotide sequences of mammalian type C helper viruses are conserved in the genomes of replication-defective mammalian transforming viruses. J. Virol. **26**:570–576.
45. **Verma, I. M.** 1978. Genome organizations of RNA tumor viruses. I. In vitro synthesis of full-genome-length single-stranded and double-stranded viral DNA transcripts. J. Virol. **26**:615–629.
46. **Weinberg, R. A.** 1977. Structure of the intermediates leading to the integrated provirus. Biochim. Biophys. Acta **473**:39–61.
47. **Witte, O. N., N. Rosenberg, M. Paskind, A. Shields, and D. Baltimore.** 1978. Identification of an Abelson murine leukemia virus-encoded protein present in transformed fibroblast and lymphoid cells. Proc. Natl. Acad. Sci. U.S.A. **75**:2488–2492.
48. **Yoshimura, F. K., and R. A. Weinberg.** 1979. Restriction endonuclease cleavage of linear and closed circular murine leukemia viral DNAs: discovery of a smaller circular form. Cell **16**:323–332.